

RESEARCH

Open Access



Experimental and Analytical Investigation of the Fatigue Flexural Behavior of Corroded Reinforced Concrete Beams

Li Song^{1,2}, Zhiwei Fan¹ and Jian Hou^{3*}

Abstract

The fatigue flexural behavior of corroded reinforced concrete (RC) beams was experimentally and analytically examined. Seven beams were constructed and tested, and an analytical fatigue prediction model (FPM) was proposed to assess the fatigue behavior of the corroded beams. After validating the FPM with the experimental test results, the FPM was then extended to better understand the effects of the degree of steel corrosion, the corrosion pit geometry, and the fatigue load level on the performance of corroded RC beams. The results show that the fatigue behavior of the corroded steel bars determines the fatigue behavior of the beams. Rebar corrosion has a significant detrimental effect on the fatigue performance of RC beams due to stress concentration, loss of steel cross-sectional area, and diminished bonding at the steel–concrete interface. The stress concentrations increase with increasing pit width-to-length and depth-to-diameter ratios. Differences in pit geometry and the resulting changes in stress concentrations due to corrosion should be considered when assessing fatigue performance.

Keywords: fatigue flexural behavior, reinforced concrete beam, experiment, fatigue prediction mode, corrosion, pit geometry, stress concentration

1 Introduction

The corrosion of reinforcing bars is a major factor that affects the deterioration of reinforced concrete (RC) structures; corrosion is typically associated with chloride ingress and carbonation (Ma et al. 2014; Coronelli and Gambarova 2004). Structural corrosion causes a loss of steel area, reduced reinforcement strength, cracking and spalling of the concrete cover, and diminished bonding at the steel–concrete interface (Almusallam 2001; Masoud et al. 2001; Ai-Hammoud et al. 2010). Structures such as highway and railway bridges are subjected to cyclic loading over their service lives, and this repeated stress can result in fatigue damage to the material. Although considerable effort has been expended on studying corrosion and fatigue, few studies have considered the coupled

effect of these two processes (Ai-Hammoud et al. 2011; Yi et al. 2010). Several studies have shown that localized corrosion that leads to pitting may provide sites for fatigue crack initiation and that corrosive agents can increase the growth rate of fatigue cracks (Bastidas-Arteaga et al. 2009; Bigaud and Ali 2014). The coupled action of corrosion and fatigue is more damaging than the sum of the damage caused by each component individually. Additionally, the strength and stiffness losses can be exaggerated if corrosion is combined with fatigue loading (Ai-Hammoud et al. 2011). Therefore, the repair and maintenance of bridges exposed to both corrosion and fatigue is a critical issue in long-term infrastructure durability.

The fatigue behavior of corroded concrete girders has recently received increased attention due to the increasing deterioration rate of bridges and the need to restore girder integrity to within an acceptable margin of safety under applied mechanical fatigue loading. In the laboratory, rebar that has been corroded by natural and accelerated processes has been tested with tensile fatigue

*Correspondence: houjian0323@126.com

³ Department of Civil Engineering, Xi'an Jiaotong University, Xi'an 710049, China

Full list of author information is available at the end of the article

Journal information: ISSN 1976-0485 / eISSN 2234-1315

loading, and the results have indicated notable reductions in fatigue strength and fatigue life along with a significant degradation in ductility. Empirical formulas have also been proposed to evaluate the fatigue strength of corroded rebar (Zhang et al. 2012). Yi et al. (2010) tested corroded beams under flexural fatigue loading and concluded that the corrosion of steel reinforcement decreases the fatigue life and fatigue capacity of beams and causes brittle failure. Masoud et al. (2001) tested corroded beams and beams strengthened with carbon fiber reinforced polymer (CFRP) sheets under repeated loading and concluded that the corrosion of the steel reinforcement decreased the fatigue life of beams. Repairing the beams with FRP decreased the tensile stress in the steel reinforcement and increased the fatigue life of the beams.

In most studies, corroded and uncorroded beams exhibit the same mode of failure: the fracturing of the tensioned steel reinforcement. The fatigue life of an RC beam is dependent on the fatigue behavior of the tensioned reinforcing steel. Thus, most prediction models of fatigue life for corroded RC beams are based on fatigue models of corroded reinforcement. The most common approaches are the stress-life and strain-life methods (Ma et al. 2014; Elrefai et al. 2012). Ma et al. (2014) developed a theoretical model based on fracture mechanics for aging RC beams subjected to cyclic bending. The proposed method couples the corrosion growth kinetics and fatigue crack growth kinetics. Bastidas-Arteaga proposed a mechanical model for corrosion fatigue that considers corrosion pit growth and the transition to fatigue crack growth as the primary mechanisms (Bastidas-Arteaga et al. 2009). In real structures, corrosion pits act in a manner similar to notches because pitting geometry is not identical to mathematically sharp cracks; the notches interact with the fatigue cracks. Few studies have considered how different corrosion pit shapes affect the fatigue strength of deformation bars.

Fatigue loading can weaken one or more individual system components (corroded steel and concrete) and deteriorate the bond. Many researchers have noted that the fatigue performance of corroded RC beams is not well documented and needs further research. The differences in accelerated corrosion techniques and the variations in corrosion pit geometry have resulted in contradictory test data. Song and Yu (2015), Song and Jian Hou (2017) proposed an analytical fatigue prediction model (FPM) to assess the fatigue behavior of the CFRP-strengthened corroded beams; they concluded that the fatigue behavior of the corroded steel bars is the controlling factor for the fatigue behavior of the CFRP-strengthened corroded beams and that corrosion of the steel negatively affects the fatigue behavior of the beam. In this study, only the

average corrosion degree was considered, and the corrosion pit patterns on the steel surface were neither measured nor studied. In the past, both natural and artificially accelerated corrosion programs have been used to develop corrosion of the rebars in RC beams. Each of these approaches has inherent strengths and shortcomings and hence should be considered as complementary to each other. Despite artificially accelerated corrosion programs being limited in characterization of corrosion mechanism and process, they can be improved using natural corrosion methods, and can form a strong foundation for the effect steel corrosion on concrete structures and applicability. The main challenges still remaining are the development of FPM in corroded concrete structures (accelerated and natural corrosion) and the quantification of effect the geometry of corrosion pits on concrete structures. Differences in the pit geometry and the resulting changes in the stress concentration due to corrosion were not investigated. In addition, the effect of corrosion pit geometry on fatigue behavior was not studied.

This paper closes the gaps found in the literature by examining the following:

- RC beams subjected to low corrosion (0 to 5% average mass loss), medium corrosion (5 to 10% average mass loss) and high corrosion (10 to 25% average mass loss);
- Corrosion pit patterns with increasing corrosion degree;
- The effect of corrosion pit geometry on the stress concentration factor; and
- The FPM used to assess the fatigue behavior of the corroded beams considering the effect of the corrosion pit geometric parameters on fatigue behavior.

The objective of this study is to investigate the flexural fatigue behavior of corroded RC beams and to develop a new fatigue prediction model (FPM) for corroded RC beams based on the fatigue properties of the constituent materials and the cross-sectional stress redistribution. This FPM can be used to assess the failure mode, fatigue life, fatigue stiffness, and post-fatigue capacity of corroded beams under fatigue loading.

2 Experimental Program

The experimental program used in this study consisted of seven RC beams. All beams were of the same size with a cross section of 120×200 mm and a length of 1500 mm. The typical geometry and reinforcement of the beams are shown in Fig. 1. All beams were simply supported with a span of 1200 mm and loaded at two symmetrical third-point loads. The 28-day average compressive strength of the prism concrete was 24.3 MPa. The actual

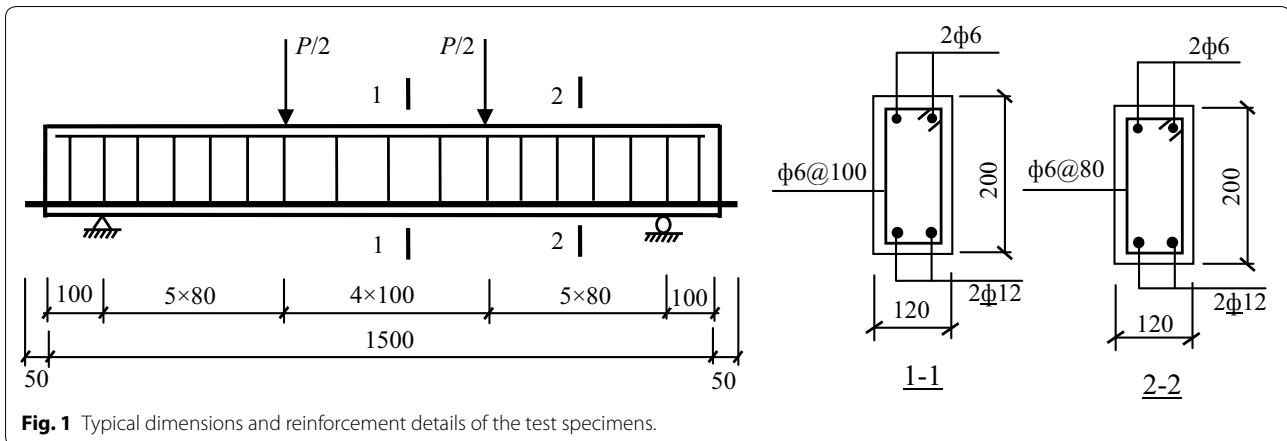


Fig. 1 Typical dimensions and reinforcement details of the test specimens.

yield strength and the ultimate strength of the 12-mm diameter deformed bars were 385.0 and 540.0 MPa, respectively.

An artificially accelerated corrosion program was used to induce corrosion damage in the test specimens within a reasonable amount of time. The beams were immersed in a 3.0% sodium chloride solution in a tank with the rebar positioned slightly above the solution. To accelerate the corrosion process, the beams were subjected to a current density of 200 $\mu\text{A}/\text{cm}^2$. The two tensioned steel reinforcement bars were then connected to the positive terminal of a DC galvanostatic power supply; a copper bar placed in the solution was connected the negative terminal. The severity of beam corrosion was controlled by Faraday’s law (Chung et al. 2008). The current density and times were monitored during corrosion. The applied current density was kept at approximately 200 $\mu\text{A}/\text{cm}^2$ during the accelerated corrosion process. In compliance with Faraday’s law, different durations of impressed current were employed to achieve various degrees of corrosion of the rebars in the beams. The estimated corrosion times for beams with average corrosion degrees of 5.0%, 10.0%, 15.0%, and 20.0% were 25, 50, 75 and 100 days, respectively. The severity of corrosion varied from low corrosion (0 to 5% average mass loss) and medium

corrosion (5 to 10% average mass loss) to high corrosion (10 to 25% average mass loss). The actual corrosion degree of the steel reinforcement was determined using the mass loss, as described in the ASTM standard G1-03 designation C3.5 (ASTM G1-03, 2003).

Prior to casting the beams, strain gauges were attached to the tensioned reinforcing steel at the midspan of the beam. Prior to testing, five concrete strain gauges were installed on the concrete surface at the midspan across the height of the beam. Deflections in the beams were recorded using five linear variable displacement transducers (LVDTs). Three of the LVDTs were mounted at the midspan and 200 mm to each side of the midspan to record the vertical displacement. The two remaining LVDTs were mounted on the top face of the beam above the supports at both ends to record the vertical displacements and thus account for the support settlement of the beams.

Table 1 shows a summary of the specimens and loading conditions. As a reference, one beam was neither corroded nor fatigue loaded. The remaining six beams were corroded to different degrees (low, medium, and high) to simulate damage caused by aggressive environments and were then cyclically tested to the point of failure. The relevant committees recommend a maximum

Table 1 Summary of the specimens and loading conditions.

Specimen	Corrosion degree (%)	Applied load at yield, and ultimate P_y , and P_u (kN)	Fatigue load P_{min}/P_{max} (kN)	Fatigue life, N (10^4)	Mode failure
Beam 1	0.0	69, 76	–	–	Monotonic
Beam 2	0.0	–	10/35	275.6	Steel rupture
Beam 3	4.5	–	10/35	95.3	Steel rupture
Beam 4	7.2	–	10/35	48.7	Steel rupture
Beam 5	12.1	–	10/35	16.2	Steel rupture
Beam 6	17.7	–	10/35	2.3	Steel rupture
Beam 7	21.3	–	10/35	4.0	Steel rupture

stress range of 125–165 MPa for straight deformed bars, such as 138 MPa according to ACI Committee 215 and 150 MPa according to CEB-FIP and China Code for design of concrete structures. The fatigue load levels in the manuscript were selected based on the stress range of the longitudinal reinforcing bars in the uncorroded Beam 2. The maximum load P_{\max} and minimum load P_{\min} in the fatigue load cycles were 46.0% (35 kN) and 13.1% (10 kN), respectively, of the maximum static load capacity of the reference beam. The locations of the two loading points are shown in Fig. 1.

3 Discussion of Experimental Results

3.1 Failure Modes

When submitted to fatigue loading, both the uncorroded and corroded beams exhibited the same mode of failure—fracturing of the tension steel reinforcement (Fig. 2). Under repeated loading, short flexural cracks formed at the bottom of the beam during the first few hundred cycles and then propagated to intersect with a longitudinal corrosion crack that occurred at the same height as the tension steel reinforcement. Some flexural cracks that crossed the longitudinal crack propagated toward the center of the beam, whereas several of the new

cracks propagated vertically from the edges of the longitudinal crack as the number of applied cycles increased (Fig. 2). In addition, bond deterioration between the steel and the surrounding concrete increased the maximum crack width and the deflection. Higher levels of stress can develop in the steel bars at the crack locations. The fatigue crack in the steel bar originated from the corrosion pit on the bar's deformed surface; the presence of significant stress concentrations at the corrosion pit locations led to the fracturing of the bar. In the corroded beams, the fatigue failure of the reinforcing bar was accompanied by a sudden extension of the flexural cracks followed by crushing of the upper concrete layers.

3.2 Corrosion Pit Patterns

Corrosion pits, similar to mechanical notches on the surface of steel reinforcement bars, tend to intensify local stress fields. The magnification of the local stress field can be expressed by the stress concentration factor (SCF), which is dependent on the geometry of the notch. Corroded rebar was obtained from post-fatigue RC beams, and the geometry of typical corrosion pits on the rebar was measured using KH-7700 Motor 3D Video Microscope. Figure 6 shows the relationships

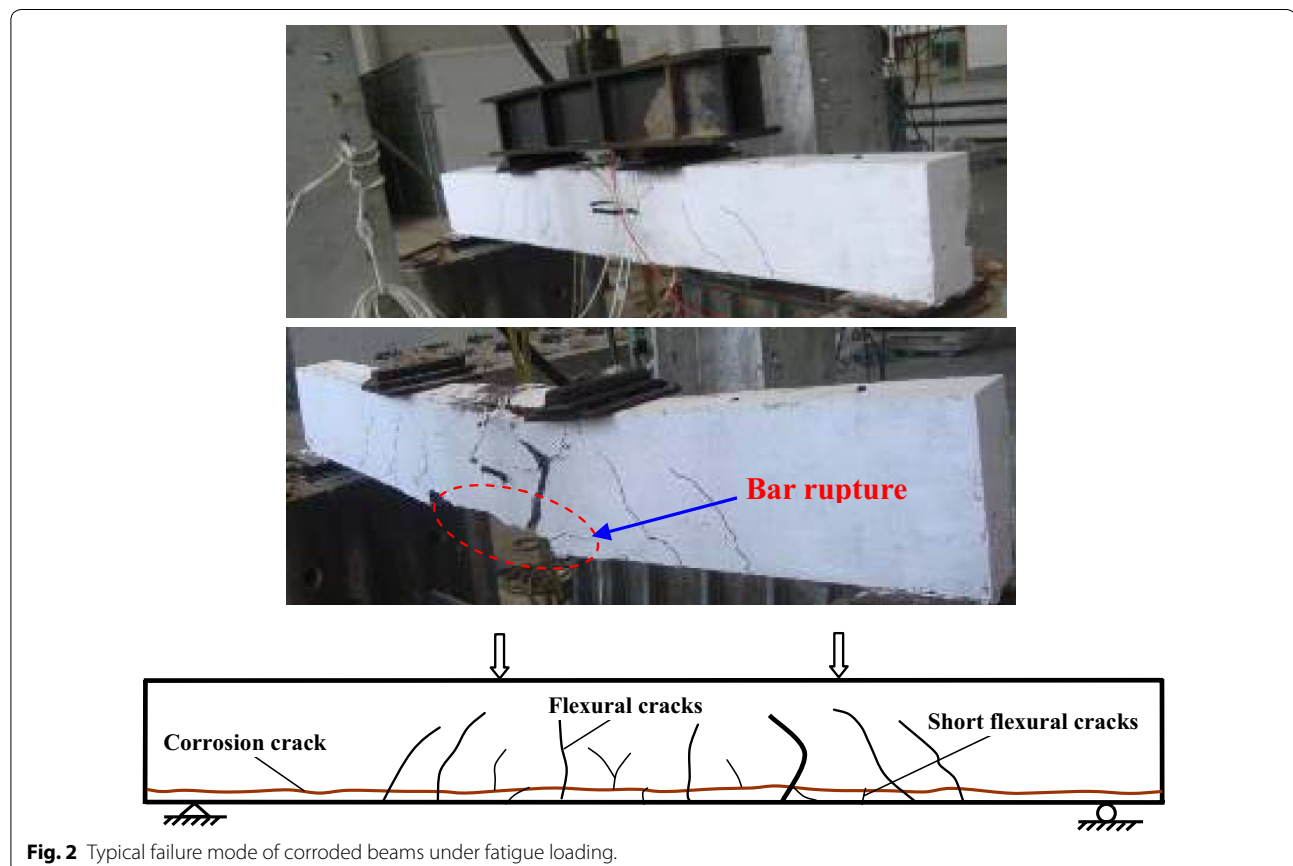


Fig. 2 Typical failure mode of corroded beams under fatigue loading.

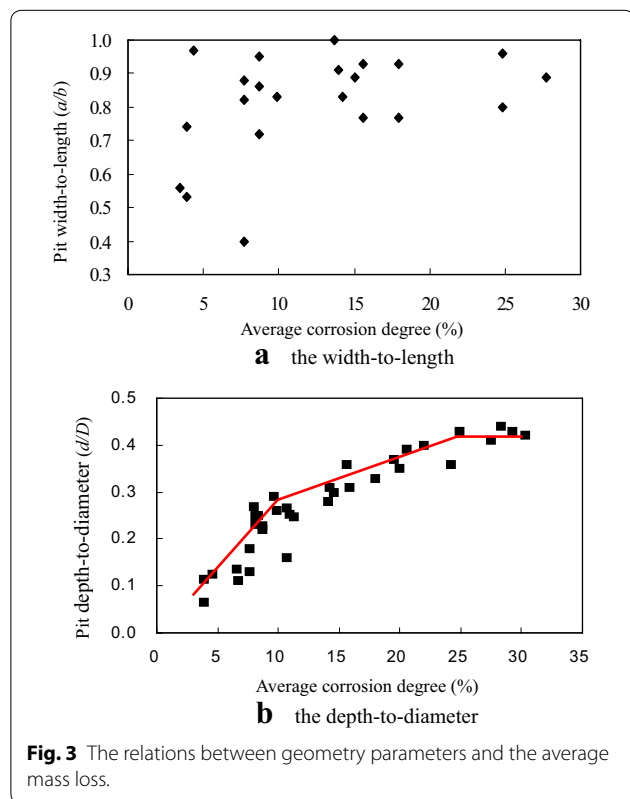
between the geometric parameters and the average mass loss. The non-uniform corrosion patterns make it difficult to accurately quantify the effects of the corrosion degree on the width-to-length ratio (a/b); however, most of the data are within the range of 0.5–1.0 (Fig. 3a). The maximum depth-to-steel diameter (d/D) initially increased rapidly followed by a slow increase at high degrees of corrosion and then a stable region in which the depth-to-steel diameter remained relatively constant as corrosion progressed (Fig. 3b).

The test results show that pitting of the steel reinforcement due to corrosion occurred only after an approximately 3.5–5.0% actual mass loss and that the initial corrosion pits tended to act as sharp notches on the surface of the steel bar. The pit depth increased with increasing corrosion degree, and the pit lengths in the longitudinal and transverse directions increased at higher rates. The pit depth then increased slowly, and corrosion developed primarily along a circle similar to carbonation-induced uniform corrosion. From a mechanical perspective, a deep, sharp pit has a larger SCF, and a long, shallow pit has a smaller SCF. This observation indicates that there was an initially rapid increase in the SCF (slight corrosion) followed by a stable increase (medium corrosion) and then a stable

region, in which the SCF remained relatively constant at higher degrees of corrosion (severe corrosion).

3.3 Fatigue Life

The fatigue life (Table 1) decreased by 65.4%, 82.3%, 94.1%, and 98.5% of that of control Beam 1, accompanied by mass losses of 4.5%, 7.2%, 12.1%, and 21.3%, respectively. A 1% increase in the degree of corrosion reduced the fatigue life by 14.5% at 4.5% corrosion, by 11.4% at 7.2% corrosion, and by 4.6% at 21.3% corrosion. In the test, the geometry of the corrosion pits and reduction of the steel area were measured, and the bond deterioration was assessed using the strain between reinforcing bars and the surrounding concrete in the cross section. Figure 3b shows that at the maximum corrosion depth, there was approximately 3.5% actual mass loss, followed by an initial rapid increase, and then a slow increase at high corrosion degrees and finally a stable region where the corrosion depth remained relatively constant as corrosion progressed. For the bond strength, an initial increase for limited corrosion levels (precracking stage) is followed by a decrease because of the concrete cover splitting as a result of corrosion-induced cracking. The test results show that the decrease in fatigue life is attributed to the following three primary factors: stress concentrations from the formation of corrosion pits, reduction of the steel area caused by corrosion, and bond deterioration at the steel–concrete interface due to the coupled effect of corrosion and fatigue. At low degrees of corrosion (0 to 5% average mass loss), there is an initial increase or slight decrease in the bond strength and a slight decrease in steel area; however, the fatigue life decreased by 65.4% compared to that of the uncorroded beam at 4.5% mass loss, meaning that the decrease in fatigue life is attributed to the stress concentration from the formation of corrosion pits. At medium degrees of corrosion (5 to 10% average mass loss), there is a rapid increase in pit depth, a significant deterioration of bond strength and a reduction of steel area; the fatigue life was reduced by 82.3% compared to that of the uncorroded beam at 7.2% mass loss, meaning that the decrease in fatigue life is attributed to the three previously mentioned factors. At high degrees of corrosion (10 to 25% average mass loss), there is a slow increase in pit depth, a relative stable bond strength and a significant reduction of steel area; the fatigue life was reduced by 98.5% compared to that of the uncorroded beam at 21.3% mass loss, meaning that the decrease in fatigue life is primarily due to the reduced cross-sectional area of the bar.



4 Fatigue Prediction Model

As mentioned in the introduction, the other objective of this study is to develop a new FPM of corroded RC beams based on the fatigue properties of the constituent materials and cross-sectional stress analysis. This section introduces the implementation procedure of the prediction model.

4.1 Fatigue Properties of Constituent Materials

To predict the fatigue behavior of a composite member, first, the effects of cyclic loading on its constituent components must be understood. The fatigue properties of concrete and corroded steel bars are examined first, and the effect of the corrosion pit geometric parameters on the stress concentration is then studied using the finite element method.

4.1.1 Concrete

The concrete creep in compression was evaluated using the cumulative residual strain of concrete in compression at predetermined fatigue cycles. The beam test results showed that the concrete creep in the compression zone subjected to repeated loading was a significant factor for increasing the steel tensile stress and the deflection. The accepted principle implies that the concrete strain ε_c under cyclic loading is the sum of the strain under sustained loading ε_{ce} plus the strain increment (creep strain) ε_{cr} under cyclic loading (Holmen 1982). The strain increment depends on loading conditions, such as the stress range and the number of cycles, and describes the irrecoverable portion of the deformation. The strain increment under cyclic loading is as follows (China Academy of Building Research 1994):

$$\varepsilon_{cr} = \frac{f_c}{E_c} n^{0.29} \lg^{-1} (3.29\alpha_r - 4.66) \quad (1)$$

where n is the number of loading cycles, f_c is the concrete compressive strength, E_c is the initial Young's modulus of the concrete, and α_r is the stress ratio coefficient as derived from Eq. (2):

$$\alpha_r = \frac{\sigma_{c,max} - \sigma_{c,min}}{f_c - \sigma_{c,min}} \quad (2)$$

where $\sigma_{c,min}$ and $\sigma_{c,max}$ are the minimum and maximum stresses in the concrete.

The Young's modulus of the concrete under repeated loading is estimated as follows:

$$E_c^f = \frac{\sigma_{c,max}}{\varepsilon_{ce} + \varepsilon_{cr}} \quad (3)$$

The Young's modulus of the concrete in the n th load cycle can thus be derived from Eqs. (1) and (3):

$$E_c^f(n) = \sigma_{c,max} / \left\{ \frac{\sigma_{c,max}}{E_c} + \frac{f_c}{E_c} \times n^{0.29} \lg^{-1} (3.29\alpha_r - 4.66) \right\} \quad (4)$$

Fatigue loading induces the propagation of internal micro-cracks in the concrete, significantly increasing the irrecoverable strain. The strain increment during the fatigue life of concrete in compression increases rapidly during the initial cycles, after which it tends to stabilize just prior to the end of the fatigue life. The critical point of concrete failure is estimated as follows (China Academy of Building Research, 1994):

$$\varepsilon_{cr} \geq 0.4f_c/E_c \quad (5)$$

4.1.2 Corroded Steel Bars

Extensive research results show that the fatigue behavior of steel reinforcement primarily depends on the stress range and the maximum stress limit. The pitting corrosion of the steel bars increases the effective stress as a result of reducing the steel area and stress concentration in the corrosion pits. The increased localized effective stress results in the fracture of the corroded steel bars at a lower fatigue life than those of identical uncorroded steel bars. Localized corrosion that leads to pitting also provides sites for fatigue crack initiation. The cross section of the steel bars diminishes with the growth of the fatigue crack, and at some locations, the effective stress reaches the yield point. Therefore, the evolution of the steel bar cross-sectional area during fatigue life can effectively denote fatigue damage properties. The residual area of the corroded rebar to fracture is determined as follows:

$$A_s^f(N) = \sigma_{s,max} \cdot A_{sc}/f_{yc} \quad (6)$$

where N is the number of cycles to failure, $A_s^f(N)$ is the residual area of the corroded rebar in the N th load cycle, A_{sc} is the area of the corroded rebar, $\sigma_{s,max}$ is the maximum applied nominal stress on the rebar, and f_{yc} is the yield strength of the corroded rebar.

Because the stress amplitudes during the fatigue life in most structures are lower than the steel yield stress, the mechanism of elastic fatigue is responsible for the steel fracture. Thus, the damaged area is assumed to have a linear relationship with the number of load cycles. The residual area of the corroded steel $A_s^f(n)$ in the n th load cycle can be estimated as:

$$A_s^f(n) = A_{sc} [1 - (n/N) \cdot (1 - \sigma_{s,max}/f_{yc})] \quad (7)$$

The yield strength of corroded rebar can be expressed in terms of the strength of uncorroded rebar and the corrosion degree as follows (Song 2008):

$$f_{yc} = \frac{1 - 1.196\eta_s}{1 - \eta_s} f_{y0} \quad (8)$$

where f_{y0} and f_{yc} are the yield strength of the uncorroded and corroded rebar, respectively, and η_s is the average degree of rebar corrosion.

In Eq. (7), the fatigue life is calculated using the stress-life equation regressed from the constant-stress-amplitude fatigue test of steel samples at $\rho = 0.1$ (where $\rho = \sigma_{s,min}/\sigma_{s,max}$) (Song 2008):

$$\log N = (24.427 + 3.4\eta_s) - (7.6597 + 2.1\eta_s) \log \Delta\sigma \tag{9}$$

where $\Delta\sigma = (\sigma_{max} - \sigma_{min})$ is the nominal stress range and is determined by the first cycle.

The test results of the corroded beams show the stress concentration induced by concrete cracks and pitting corrosion; the stress ratio significantly influences the localized effective stress in the rebar. Thus, the stress-life curve of corroded rebar in RC beams can be rewritten as:

$$\begin{aligned} \log N = & (24.427 + 3.4\eta_s) \\ & - (7.6597 + 2.1\eta_s) \\ & \log K_L K_f (K_\rho - \rho) \sigma_{max} \end{aligned} \tag{10}$$

where K_ρ is the fatigue strength factor caused at the stress ratio ρ , K_L is the stress concentration factor induced by flexural cracks of the concrete, and K_f is the stress concentration factor caused by corrosion pits in the rebar. The values of K_ρ , K_L , and K_f are calculated below.

The fatigue strength factor K_ρ can be calculated as follows (Song 2006):

$$K_\rho = \frac{0.938}{1 - 0.6165\rho} \tag{11}$$

The experimental results show that the localized stresses in the tensioned steel reinforcement at the concrete cracks were higher than the nominal values. Hefferan et al. similarly found that localized stresses were consistently 20–40% greater than the average stresses (Hefferan et al. 2004). In this study, the stress concentration factor K_L was applied to modify the effect of flexural cracks in the concrete on the localized stresses of the steel bar. An average value of $K_L = 1.25$ was selected.

Several methodologies such as experimental measurements and the finite element method have been proposed to calculate the SCF (Nakamura and Suzumura 2013). However, it is difficult to accurately measure the SCF of corrosion pits experimentally. In this study, the stress concentration effect of corrosion pits was investigated using finite element stress analysis. Several studies

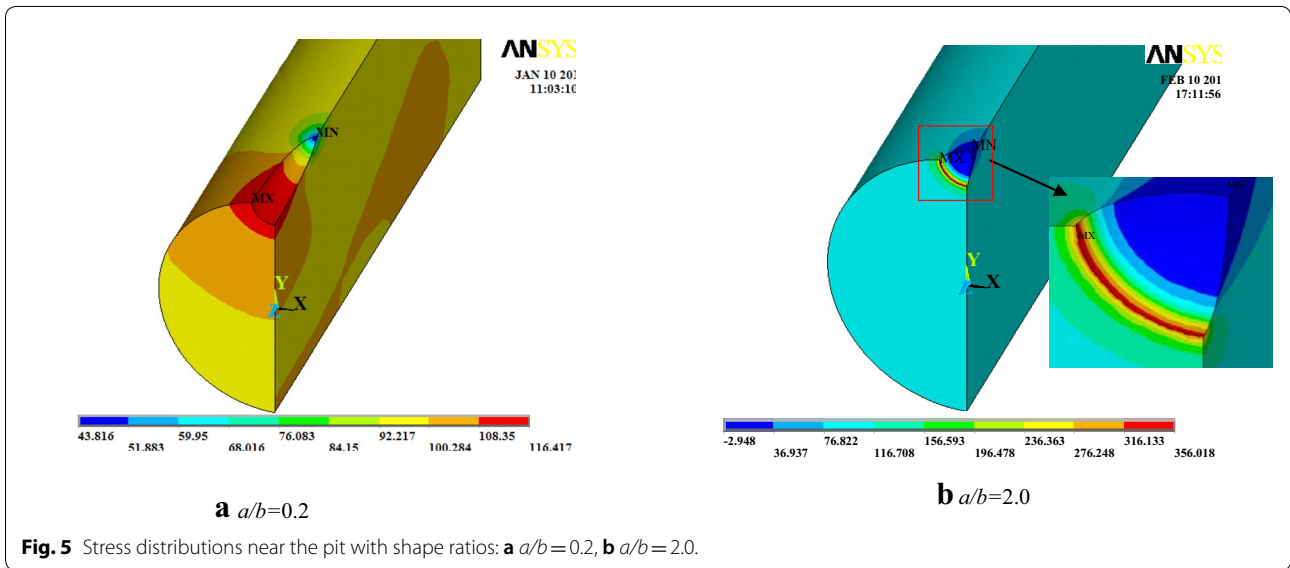
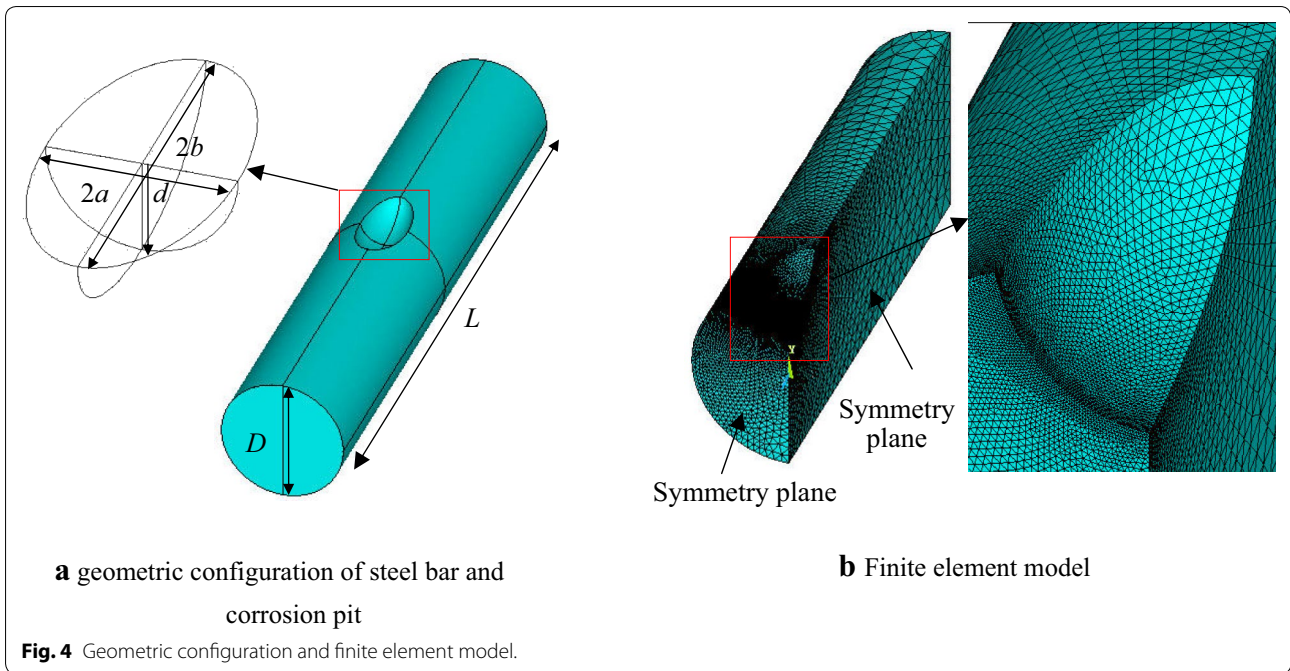
have reported corrosion pits with different shapes such as dish-shaped pits, round semi-spherical pits, and semi-ellipsoidal pits (Ceri et al. 2009; Huang et al. 2014; Kashani et al. 2013; Tang et al. 2014). This study simplified the corrosion pits as semi-ellipsoids. The stress concentration effects of single semi-elliptical pits with different geometries were investigated for uniaxial loading by systematically conducting a series of 3D stress analyses. An equation to estimate an SCF that depends on geometric parameters was developed based on the results of the stress analyses.

A finite element stress analysis model was developed using ANSYS 12 software to simulate the stress state near the idealized pit, which was located on the surface and at the center of a reinforcing bar with a length (L) and diameter (D) (Fig. 4a). In the coordinate system, a pit length of $2b$ was defined as the dimension of the pit in the loading direction, a pit width of $2a$ was defined as the dimension perpendicular to the loading direction, and the pit depth was d . The modulus of elasticity and Poisson’s ratio were taken as 200 GPa and 0.3, respectively. A uniform stress of 100 MPa was applied to the end of the 20-mm diameter steel bar. Due to the symmetry of the model, only one-quarter of each steel bar was modeled (Fig. 4b). The SCF was calculated using the ratio of the maximum tensional stress to the nominal tensional stress.

Figure 5 shows the stress distributions for width-to-length ratios of $a/b = 0.2$ and $a/b = 2.0$ for $d = 2$ mm. The stress contour shows that the stress concentration is located near the pit and narrows gradually with increasing values of a/b . The maximum stress region is near the intermediate cross section of the pit in the tension direction. The maximum stress occurs at the intersection of the surface of the steel bar and the intermediate cross section of the pit, and the minimum stress occurs at the ends of the pit in the tension direction.

Figure 6 summarizes the SCF as a function of the corrosion pit shape ratios for $d/D = 0.05–0.5$ and $a/b = 0.5, 0.7, \text{ and } 1.0$. For a pit with a given ratio of a/b , the SCF increases rapidly with d/D , particularly at higher ratios of a/b . The experimental results (Fig. 6b) show that the d/D ratio becomes stable when the degree of corrosion becomes severe, meaning that the SCF tends to become approximately constant. An empirical equation that quantitatively correlates the SCF to the pit shape ratio a/b and the degree of corrosion η_s based on the experimental and numerical results can be expressed as follows:

$$K_f = \begin{cases} 1.0 + 8.4(a/b)^2 \eta_s & (\eta_s \leq 5\%) \\ 1.0 + 0.42(a/b)^2 + 3.15(a/b)(\eta_s - 0.05) & (5\% < \eta_s \leq 25.0\%) \\ 1.0 + 0.63(a/b) + 0.42(a/b)^2 & (\eta_s > 25.0\%) \end{cases} \tag{12}$$



Based on the calibration results between the corroded pit depth and the fatigue life of the corroded beams, Ai-Hammoud et al. (2011) recommends the following SCF values: 1.78–2.15 for slightly corroded beams, 1.78–2.28 for mildly corroded beams, and 1.87–2.89 for highly corroded beams. Ma et al. (2014) recommends an expression and SCF values as follows: 1.0–2.1 for slightly corroded beams, 2.1–1.54 for mildly corroded beams, and 1.54–1.30 for highly corroded beams. The scatter of the SCF values is attributed to not only the different accepted

corrosion techniques but also the variety of corrosion pit shapes. Unlike the depth of corrosion pits, the effect of corrosion pit shapes (width-to-length ratios) on the SCF has not yet been fully addressed.

The fatigue damage process of a steel bar is a lengthy process. Corrosion pits provide sites for fatigue crack initiation, and then fatigue crack evolution under repeated loading further reduces the cross-sectional area of the bar. With the growth of the fatigue cracks, the effective stress reaches the yield point at some locations. The bar

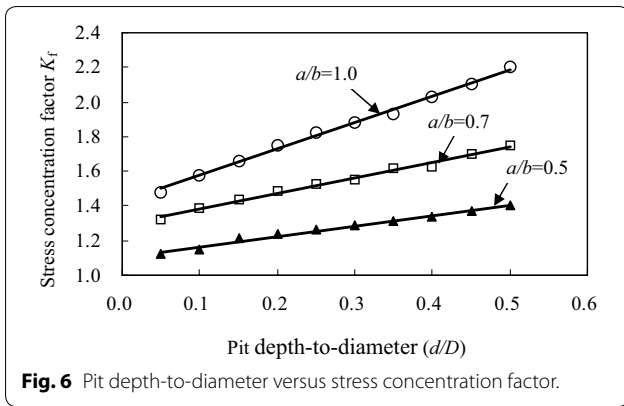


Fig. 6 Pit depth-to-diameter versus stress concentration factor.

is assumed to abruptly break when the localized stress of the bar $\sigma_{s,max}^f$ reaches the yield stress, as given in Eq. (13):

$$\sigma_{s,max}^f \geq f_{yc} \tag{13}$$

4.2 Cross-Sectional Stress Analysis

The test results showed that bond deterioration between the corroded rebar and concrete significantly contributed to increased crack width and deflection under cyclic loading. In addition, the relative slippage between the corroded rebar and concrete caused the strain distribution across the depth of the beam to be nonlinear. Thus, bond deterioration properties under cyclic loading should be considered in the fatigue prediction model. Oudah and El-Hacha (2013) developed a simplified method to assess the effect of bond degradation on strain distribution. The form of the compatibility equation of strain in the RC beams can be written as follows:

$$\epsilon_s = \left(\frac{h_0 - x_n}{x_n} \right) \epsilon_c \gamma_s \tag{14}$$

where ϵ_c is the concrete strain at the top fiber, ϵ_s is the strain in tensioned steel at a cracked section, x_n is the depth from the top fiber to the neutral axis, h_0 is the depth from the top fiber to the level of the tensioned steel, and γ_s is the strain compatibility factor for steel. Based on the test results of concrete strain ϵ_c , steel strain ϵ_s , and depth x_n , the strain compatibility factor γ_{sc} for corroded beams was derived by inversely solving Eq. (14). The calculated results of γ_{sc} are 1.01–0.75, 0.93–0.72, and 0.78–0.57 at average degrees of corrosion of 4.5%, 7.2%, and 21.3%, respectively. The average values of γ_{sc} can be regressed as follows:

$$\gamma_{sc} = -1.126\eta_s + 0.91 \quad (\eta_s \leq 0.25) \tag{15}$$

The strain and stress distributions over the beam depth under cyclic loading are shown in Fig. 7. It is assumed that the concrete strain in the compressive

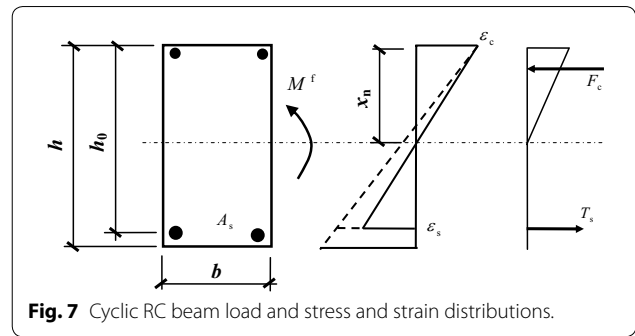


Fig. 7 Cyclic RC beam load and stress and strain distributions.

zone shows linear distribution across the depth of the beam; the tensile resistance of the concrete under the neutral axis is ignored. Based on Eqs. (14) and (15), the strain compatibility equation can be expressed as:

$$\frac{\gamma_{sc}\epsilon_c}{x_n} = \frac{\epsilon_s}{h_0 - x_n} \tag{16}$$

Equating the tensile and compressive forces yields the following relationship:

$$\frac{1}{2} E_b^f \epsilon_c b x_n = A_s^f E_s \epsilon_s \tag{17}$$

where E_b^f is the deformation modulus of concrete under cyclic loading ($E_b^f = 0.61E_c^f$). Equating the internal moment and the external moment yields:

$$M^f = A_s^f E_s \epsilon_s \left(h_0 - \frac{x_n}{3} \right) \tag{18}$$

4.3 Fatigue Analysis Flowchart

The step-by-step procedure for implementing the developed FPM is listed in Fig. 8. Additional details of the steps are provided as follows:

- Input the loading scheme, the initial material parameters (A_s , E_s , f_{y0} , η_s , E_c , and f_c), the specimen configuration (b , h , and h_0), and the fatigue load (M^f);
- Solve the strain and stress of concrete and steel bars using Eqs. (16)–(18);
- Assess the fatigue states of the concrete and steel bar using Eqs. (5) and (13), respectively;
- Update the material properties, the deformation modulus of concrete (E_c^f), and the residual area of the corroded steel (A_s^f) using Eqs. (4) and (7), respectively. Return to step (2);
- End the program and output the information.

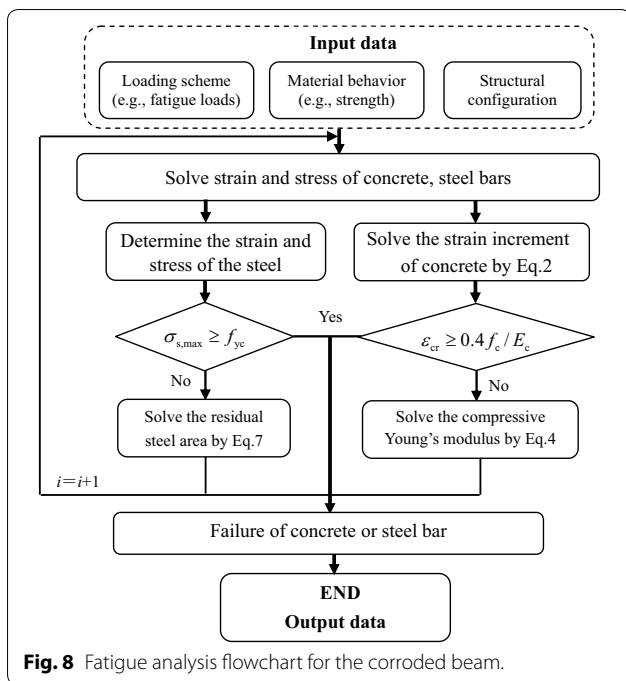


Fig. 8 Fatigue analysis flowchart for the corroded beam.

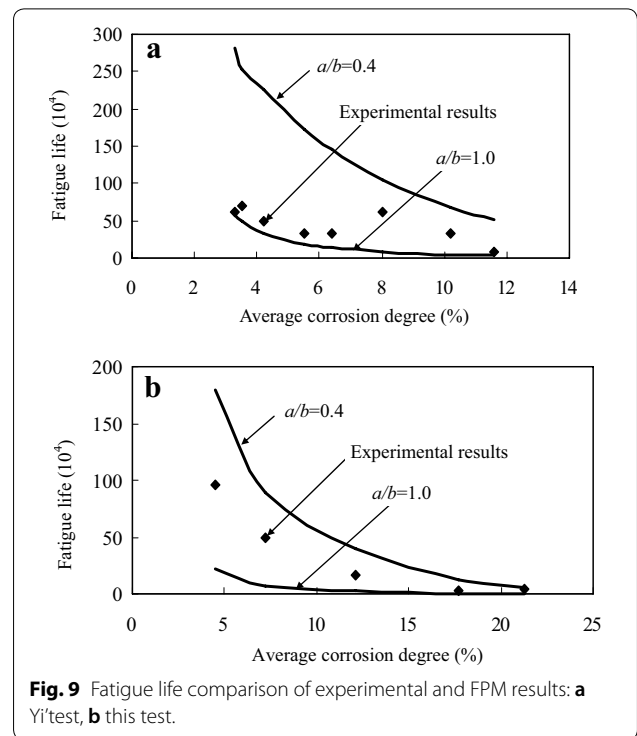


Fig. 9 Fatigue life comparison of experimental and FPM results: **a** Yi's test, **b** this test.

Table 2 Summary of the specimens and loading conditions (Yi et al. 2010).

Specimen	Corrosion degree (%)	Fatigue load P_{min}/P_{max} (kN)	Fatigue life, N (10^4)	Mode failure
BL 1	3.25	7/33	62.6	Steel rupture
BL 2	3.50	7/33	70.7	Steel rupture
BL 3	4.20	7/33	49.7	Steel rupture
BL 4	5.50	7/33	33.4	Steel rupture
BL 5	6.35	7/33	32.6	Steel rupture
BL 6	8.04	7/33	62.0	Steel rupture
BL 7	10.17	7/33	32.4	Steel rupture
BL 8	11.60	7/33	8.9	Steel rupture

4.4 Validation of the Analysis Model

In this section, the proposed FPM is validated using the experimental results of the corroded beams that were tested in this study and those of Yi et al. (2010), who tested eight beams with two deformed tensioned reinforcing bars. The beams had dimensions of 150 × 300 × 3600 mm and a span of 3400 mm. The diameter of the tensioned longitudinal rebar was 20 mm. The average compressive strength of the concrete was 22.0 MPa, and the actual yield strength and ultimate strength of the 20-mm diameter deformed bars were 390.0 and 578.30 MPa, respectively. The two tensioned steel reinforcement bars of the beams were corroded using an artificially accelerated corrosion

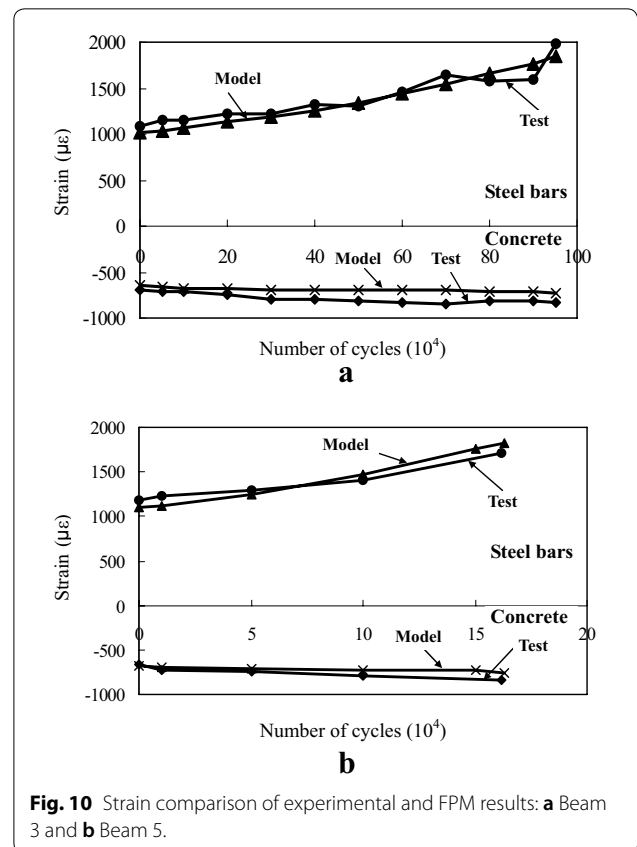
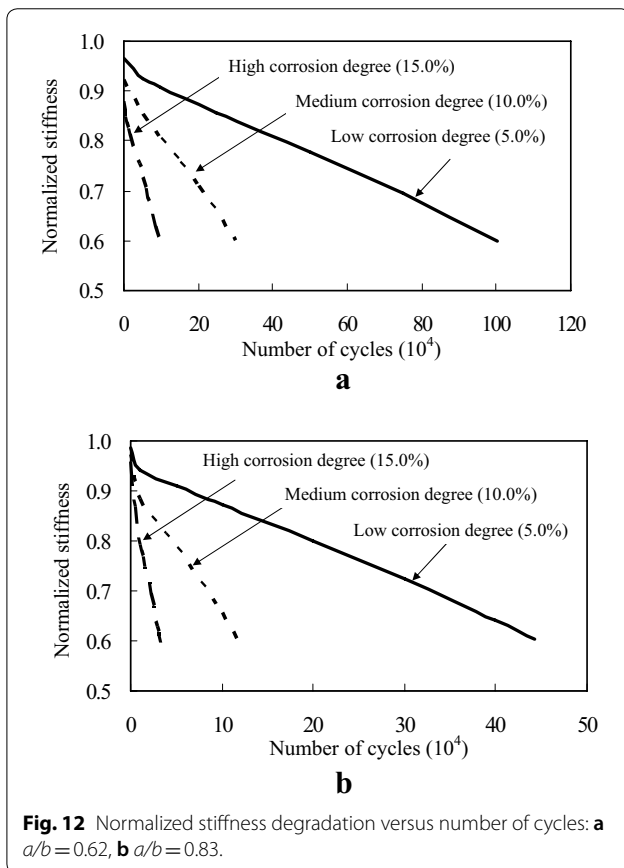
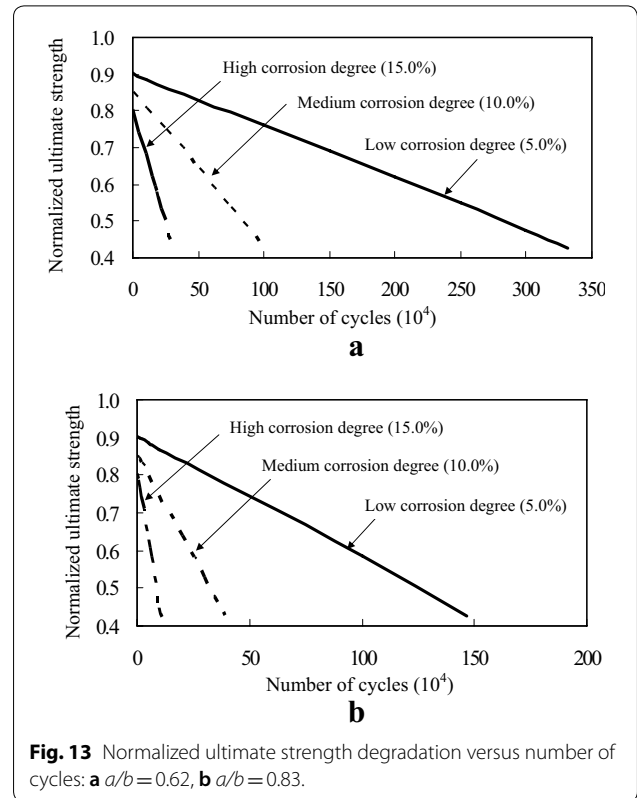
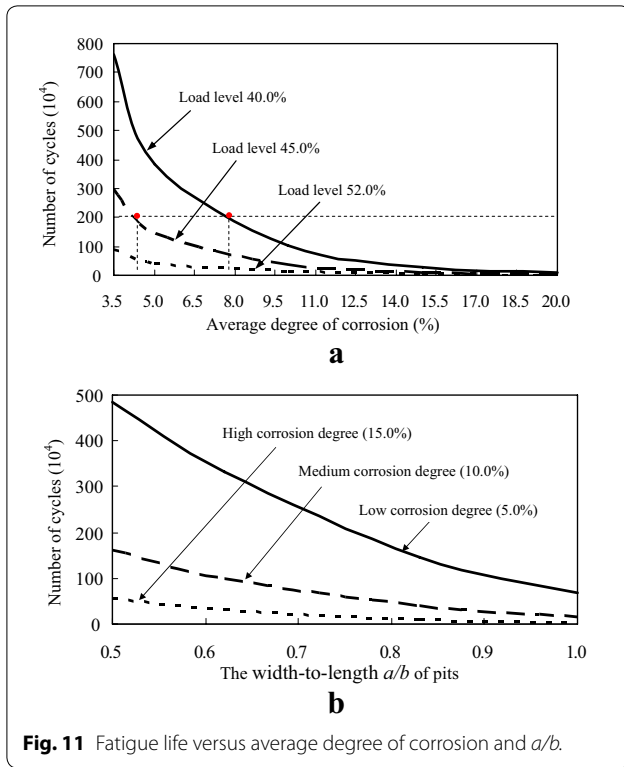


Fig. 10 Strain comparison of experimental and FPM results: **a** Beam 3 and **b** Beam 5.



program. Table 2 provides a summary of the specimens and their loading conditions.

All of the specimens failed by rupturing of the tensioned steel reinforcement, which was identical to the results of the tested specimens. Figure 9 shows the fatigue life of the corroded beams. The experimental data are between $a/b=0.4$ and $a/b=1.0$. The uncertainties of the fatigue life are caused by the geometry of the corrosion pit. As illustrated by the analysis presented above, the fatigue life of the reinforcing bars is dependent on the width-to-length ratio a/b and the depth-to-diameter ratio d/D . The predicted results correspond well with the experimental data at the average width-to-length ratio of $a/b=0.62$ in this study and $a/b=0.83$ in Yi's test, in which the geometry of the corrosion pit was associated with the artificially accelerated corrosion program.

Figure 10 shows the strain curves after different numbers of fatigue loading cycles for Beam 3 at $a/b=0.63$ and Beam 5 at $a/b=0.61$. The FPM results are consistent with the experimental data at all stages of loading to failure. The strain values in the beams are scattered because the cross section is located at the mid-section of the beams in the FPM analysis and the test measurement, whereas

the fracture cross section in the tests may not be located at the mid-section.

5 Model Application

In this section, a parametric study of the beams in Yi's test is conducted to provide a better understanding of the effects of steel corrosion, the fatigue load level, and pit geometry on the fatigue life, stiffness, and post-fatigue ultimate capacity of corroded beams.

5.1 Fatigue Life

Figure 11 shows the effect of steel corrosion on the fatigue life of beams. The fatigue life of uncorroded beams was greater than 5,000,000 cycles at a 52.0% load level, 15,000,000 cycles at a 45.0% load level, and 40,000,000 cycles at a 40.0% load level. Corrosion of the beams at corrosion levels of 5.0%, 10.0%, and 15.0% decreased the average fatigue life by 91.3%, 97.7%, and 99.8%, respectively. Corrosion levels of 4.25% and 7.75% decreased the fatigue life to 2,000,000 cycles at load levels of 45.0% and 40.0%, respectively (Fig. 13a). These results indicate that the fatigue life of beams is sensitive to the corrosion of the steel bar. Fatigue lives of 5.0% corroded beams at a 40% load level decreased by 61.9% and 88.5% when the load level increased by 5.0% and 12.0%, respectively. The fatigue lives of 10.0% corroded beams at a 40% load level decreased by 62.4% and 88.7% when the load level increased by 5.0% and 12.0%, respectively. These results demonstrate a clear influence of the load level on the fatigue life of corroded beams, and the change in the fatigue life approximately follows the same trend as that of beams with different levels of corrosion. Changing the corrosion pit shape ratio a/b from 1.0 to 0.5 increased the fatigue lives of beams at 5.0% corrosion by 6.0 times, the lives of beams at 10.0% corrosion by 8.59 times, and the lives of beams at 15.0% corrosion by 11.54 times (Fig. 13b). The fatigue lives of beams with lower levels of corrosion may be greater than those of beams with higher levels of corrosion because of the influence of the corrosion pit shape. The results clearly show that corrosion and pit shape affect fatigue life and that the load level decreases the fatigue life of beams. The decrease of fatigue life may be greater when corrosion is combined with an increase in the fatigue loading level.

5.2 Stiffness Degradation

To provide a quantitative measure of the stiffness degradation in beams, the stiffness was calculated after each fatigue loading cycle. The calculation method involved recording the strains in the tensioned steel ε_s and in the concrete at the top fiber ε_c at the mid-span section and then calculating the stiffness using the curvature radius

and fatigue load for each loading cycle. For each beam at a load level of less than 0.52, the obtained stiffness values were normalized by the initial stiffness of the uncorroded beam before applying fatigue loading, as shown in Fig. 12.

Compared with the uncorroded RC beam, the percentage decrease in the initial stiffnesses of the corroded beams was approximately 1% at 5.0% corrosion, 3% at 10.0% corrosion, and 4% at 15.0% corrosion, whereas the percentage decrease in the failure stiffnesses of the corroded beams was approximately 40.0%. These trends indicate that steel bar corrosion slightly decreased the initial stiffness and significantly increased the stiffness degradation rates. The stiffness degradation rates of the beams with $a/b=0.62$ under fatigue loading increased by an average of 3.36 times at 5.0% corrosion and 12.85 times at 10.0% corrosion. The stiffness degradation rates of the corroded beams became clearer as the a/b ratio increased. The change in stiffness is related to the opening and propagation of flexural cracks, which imply slip between the concrete and the steel reinforcement as along with failure of the concrete in the tensile zone and softening of the concrete in the compressive zone.

5.3 Post-fatigue Ultimate Strength

The ultimate strength was calculated after each fatigue loading cycle to provide a quantitative measure of the capacity degradation in the beams. The strength values were normalized by the initial ultimate strength of the uncorroded control beam before applying fatigue loading, as shown in Fig. 13.

Compared with the uncorroded RC beam, the percentage decrease in the initial ultimate capacities of the corroded beams was 10% at 5.0% corrosion, 15% at 10.0% corrosion, and 20% at 15.0% corrosion, whereas the decrease in the failure strength was approximately 57.0%. The strength degradation rates of beams with $a/b=0.62$ at a 0.45 fatigue loading level increased by an average of 3.36 times at 5.0% corrosion and 11.87 times at 10.0% corrosion. These results indicate that steel bar corrosion decreased the initial capacity and significantly increased the ultimate strength degradation rates. The strength degradation rates of corroded beams became clearer as the a/b ratio increased.

6 Conclusions

An experimental study was performed to investigate the fatigue flexural behavior of corroded RC beams. An analytical fatigue prediction model based on the fatigue properties of the constituent materials and cross-sectional stress analysis was proposed to assess the fatigue behavior of corroded beams. The following conclusions

can be drawn from the experimental and fatigue model analysis results:

1. The corroded RC beams failed due to fatigue rupture of the main corroded steel bars. The fatigue life of the beams is limited by the fatigue life of the corroded tensile reinforcing steel. The degradation of beam fatigue behavior also depends on the stress history of the tensile steel reinforcement. Thus, the controlling factor for the fatigue behavior of beams is the fatigue behavior of the corroded steel bars. The failures of both uncorroded and corroded beams were caused by rupturing of the steel reinforcement.
2. Pitting corrosion in RC beams causes increased stress concentrations, loss of steel area, and diminished bonding at the steel–concrete interface. At low degrees of corrosion, the degradation of fatigue behavior is primarily due to increased stress concentrations, while at medium degrees of corrosion, the degradation of fatigue behavior is due to all three factors. Further decreases in fatigue behavior at high degrees of corrosion are primarily due to the decreased cross-sectional areas of the steel bar.
3. Corrosion pits, which are similar to the mechanical notches on the surfaces of steel rebar, tend to intensify local stress fields. The SCF is dependent on the geometry of the corrosion pits. The width-to-length and depth-to-diameter ratios of the pits range from 0.5 to 1.0 and from 0.05 to 0.50, respectively. The SCF increased with increasing pit width-to-length and depth-to-diameter ratios.
4. Rebar corrosion has a significant detrimental effect on the fatigue performance of RC beams. The decrease in fatigue life is greater when corrosion is combined with fatigue loading. Steel bar corrosion causes a slight reduction in the initial stiffness, a significant increase in the stiffness degradation rates, a decrease in the initial load capacity, and a significant increase in the ultimate strength degradation rates.
5. Differences in pit geometry and the resulting changes in the stress concentration due to corrosion should be considered when assessing fatigue performance.

Authors' contributions

LS carried out the experiment and fatigue prediction model studies. ZF participated in the experiment studies. JH participated in the fatigue prediction model studies. All authors read and approved the final manuscript.

Author details

¹ School of Civil Engineering, Central South University, 22 Shaoshan South Road, Changsha 410082, China. ² National Engineering Laboratory for High Speed Railway Construction, Changsha 410082, China. ³ Department of Civil Engineering, Xi'an Jiaotong University, Xi'an 710049, China.

Acknowledgements

The financial support provided by National Natural Science Foundation of China (Grant Nos. 51378506, 51778631, U1434204 and 51208421) is greatly appreciated.

Competing interests

The authors declare that they have no competing interests.

Availability of data and materials

Not applicable.

Consent for publication

Not applicable.

Ethics approval and consent to participate

Not applicable.

Funding

Not applicable.

Publisher's Note

Springer Nature remains neutral with regard to jurisdictional claims in published maps and institutional affiliations.

Received: 11 February 2018 Accepted: 19 February 2019

Published online: 01 April 2019

References

- Ai-Hammoud, R., Soudki, K., & Topper, T. H. (2010). Bond analysis of corroded reinforced concrete beams under monotonic and fatigue loads. *Cement Concrete Composites*, 32(3), 194–203.
- Ai-Hammoud, R., Soudki, K., & Topper, T. H. (2011). Fatigue Flexural behaviour of corroded reinforced concrete beams repaired with CFRP sheets. *ASCE Journal of Composites Construction*, 15(1), 42–51.
- Almusallam, A. A. (2001). Effect of corrosion on the properties of reinforcing steel bars. *Construction Building Materials*, 15(8), 361–368.
- American Society for Testing and Materials. (2003). *Standard practice for preparing, cleaning, and evaluation corrosion test specimens*. West Conshohocken: American Society for Testing and Materials.
- Bastidas-Arteaga, E., Bressolette, P., Chateaufneuf, A., & Sanchez-Silva, M. (2009). Probabilistic lifetime assessment of RC structures under coupled corrosion-fatigue deterioration processes. *Structural Safety*, 31(1), 84–96.
- Bigaud, D., & Ali, O. (2014). Time-variant flexural reliability of RC beams with externally bonded CFRP under combined fatigue-corrosion actions. *Reliability Engineering & System Safety*, 131, 257–270.
- Ceri, M., Genel, K., & Eksi, S. (2009). Numerical investigation on stress concentration of corrosion pit. *Engineering Failure Analysis*, 16(7), 2467–2472.
- China Academy of Building Research. (1994). *Concrete structure research report*. Beijing: China Architectural Industry Press.
- Chung, L., Najm, H., & Balaguru, P. (2008). Flexural behavior of concrete slabs with corroded bars. *Cement Concrete Composites*, 30(3), 184–193.
- Coronelli, D., & Gambarova, P. (2004). Structural assessment of corroded reinforced concrete beams: modelling guidelines. *ASCE Journal of Structural Engineering*, 130(8), 1214–1224.
- Elrefai, A., West, J., & Soudki, K. (2012). Fatigue of reinforced concrete beams strengthened with externally post-tensioned CFRP tendons. *Construction Building Materials*, 29(4), 246–256.
- Hefferan, P. J., Erki, M. A., & DuQuesnay, D. L. (2004). Stress redistribution in cyclically loaded reinforced concrete beams. *ACI Structural Journal*, 101(2), 261–268.
- Holmen, J. O. (1982). Fatigue of concrete by constant and variable amplitude loading. *ACI Special Publication*, 75, 71–110.
- Huang, Y., Wei, C., Chen, L., & Li, P. (2014). Quantitative correlation between geometric parameters and stress concentration of corrosion pits. *Engineering Failure Analysis*, 44, 168–178.

- Kashani, M. M., Crewe, A. J., & Alexander, N. A. (2013). Use of a 3D optical measurement technique for stochastic corrosion pattern analysis of reinforcing bars subjected to accelerated corrosion. *Corrosion Science*, 73, 208–221.
- Ma, Y. F., Xiang, Y. B., Wang, L., Zhang, J. R., & Liu, Y. M. (2014). Fatigue life prediction for ageing RC beams considering corrosive environments. *Engineering Structures*, 79, 211–221.
- Masoud, S., Soudki, K., & Topper, T. (2001). CFRP-strengthened and corroded RC beams under monotonic and fatigue loads. *ASCE Journal of Composites/Construction*, 5(4), 228–236.
- Nakamura, S., & Suzumura, K. (2013). Experimental study on fatigue strength of corroded bridge wires. *ASCE Journal of Bridge Engineering*, 18(3), 200–209.
- Oudah, F., & El-Hacha, R. (2013). Analytical fatigue prediction model of RC beams strengthened in flexure using prestressed FRP reinforcement. *Engineering Structures*, 46, 173–183.
- Song, Y. P. (2006). *Fatigue behavior and design principle of concrete structures*. Beijing: China Machine Press.
- Song, L. (2008). *Fatigue flexural behaviour and fatigue life assessment for corroded RC beams strengthened with carbon fiber composite sheets*. Shanghai: Tongji University.
- Song, L., & Jian Hou, J. (2017). Fatigue Assessment Model of Corroded RC Beams Strengthened with Prestressed CFRP Sheets. *International Journal of Concrete Structures and Materials*, 11(2), 247–259.
- Song, L., & Yu, Z. W. (2015). Fatigue performance of corroded reinforced concrete beams strengthened with CFRP sheets. *Construction Building Materials*, 29(5), 99–109.
- Tang, F. J., Lin, Z. B., Chen, G., & Yi, W. J. (2014). Three-dimensional corrosion pit measurement and statistical mechanical degradation analysis of deformed steel bars subjected to accelerated corrosion. *Construction Building Materials*, 70(11), 104–117.
- Yi, W. J., Kunath, S. K., Sun, X. D., Shi, C. J., & Tang, F. J. (2010). Fatigue behavior of reinforced concrete beams with corroded steel reinforcement. *ACI Structural Journal*, 107(5), 526–533.
- Zhang, W. P., Song, X. B., Gu, X. L., & Li, S. B. (2012). Tensile and fatigue behavior of corroded rebars. *Construction Building Materials*, 34(9), 409–417.

Submit your manuscript to a SpringerOpen[®] journal and benefit from:

- Convenient online submission
- Rigorous peer review
- Open access: articles freely available online
- High visibility within the field
- Retaining the copyright to your article

Submit your next manuscript at ► [springeropen.com](https://www.springeropen.com)
